

What does chlorophyll variability tell us about export and air-sea CO₂ flux variability in the North Atlantic?

Val Bennington,¹ Galen A. McKinley,¹ Stephanie Dutkiewicz,² and David Ullman¹

Received 14 April 2008; revised 26 February 2009; accepted 18 March 2009; published 1 July 2009.

[1] The importance of biology to the ocean carbon sink is often quantified in terms of export, the removal of carbon from the ocean surface layer. Satellite images of sea surface chlorophyll indicate variability in biological production, but how these variations affect export and air-sea carbon fluxes is poorly understood. We investigate this in the North Atlantic using an ocean general circulation model coupled to a medium-complexity ecosystem model. We find that biological CO₂ drawdown is significant on the mean and dominates the seasonal cycle of pCO₂, but variations in the annual air-sea CO₂ flux and export are not significantly correlated. Large year-to-year variability in summertime pCO₂ occurs, because of changing bloom timing, but integrated bloom strength and associated carbon uptake and export do not vary substantially. The model indicates that small biological variability, quantitatively consistent with SeaWiFS (1998–2006), is not sufficient to be a first-order control on annual subpolar air-sea CO₂ flux variability.

Citation: Bennington, V., G. A. McKinley, S. Dutkiewicz, and D. Ullman (2009), What does chlorophyll variability tell us about export and air-sea CO₂ flux variability in the North Atlantic?, *Global Biogeochem. Cycles*, 23, GB3002, doi:10.1029/2008GB003241.

1. Introduction

[2] Although we can quantify the amount of carbon dioxide pumped into and remaining in the atmosphere each year, we are currently unable to fully explain why the relative magnitude of terrestrial and oceanic sinks appears to be decreasing [Raupach *et al.*, 2007; Canadell *et al.*, 2007]. The difficulty of distinguishing trends from interannual variability is one confounding factor. In order to understand the current and future trajectory of the oceanic carbon sink, the mechanisms that control its strength and year-to-year variations must be understood. Currently, direct observations at the global scale can only provide the climatological mean and seasonal cycle of the oceanic sink [Takahashi *et al.*, 2002].

[3] Ocean biology is critical to maintaining the gradient of pCO₂ between the surface ocean and atmosphere, significantly modifying air-sea gas exchange and its spatial distribution. Photosynthesis reduces oceanic pCO₂ by converting dissolved inorganic carbon (DIC) into organic carbon, and sinking organic matter creates a mass of carbon that remineralizes back to DIC at depth. This biological cycle causes a net movement of carbon from the surface to depth and is often referred to as the “biological pump.” Behrenfeld *et al.* [2006] estimate that more than one million tons of carbon is fixed into organic matter as CO₂ each day

by ocean biology. Laws *et al.* [2000] estimate that atmospheric pCO₂ would be 150–200 μatm greater than its current value if it were not for the biological control on the gradient of DIC in the ocean. It is reasonable to hypothesize that in regions of large chlorophyll blooms, interannual fluctuations in biological productivity may alter the annual sink of carbon dioxide. The subpolar North Atlantic is one such region, with a pronounced spring bloom and a large annual mean net uptake of carbon dioxide. Sabine *et al.* [2004] estimate the North Atlantic has taken up 23% of the total anthropogenic CO₂, even though it is only 15% of the global ocean surface area. Recent studies suggest this important sink may be changing. Schuster and Watson [2007], on the basis of their analysis of pCO₂ data, conclude that the North Atlantic sink between 20°N and 65°N has declined by 50% between 1994 and 2005.

[4] Coupled ocean-atmosphere model results suggest that a future increase in ocean temperatures and stratification will alter chlorophyll and export production [Sarmiento and Hughes, 1999; Bopp *et al.*, 2001]. Increases in export production in the subpolar region [Bopp *et al.*, 2001] and decreases in the subtropical region are anticipated. Behrenfeld *et al.* [2006] investigate recent (1999–2006) satellite data and suggest that global biological productivity within the subtropics has already declined, but they are unable to make any conclusions about trends in the high latitudes.

[5] To better address these ideas, we need to understand to what extent year-to-year variability of biological activity impacts the oceanic carbon sink in the present-day subpolar North Atlantic.

[6] Satellites, such as the Sea-Viewing Wide Field-of-View Sensor (SeaWiFS), provide estimates of chlorophyll at

¹Department of Atmospheric and Oceanic Sciences, University of Wisconsin-Madison, Madison, Wisconsin, USA.

²Earth, Atmospheric, and Planetary Sciences, Massachusetts Institute of Technology, Cambridge, Massachusetts, USA.

fine spatial and temporal resolution, but it is uncertain what these year-to-year variations in satellite observations mean in terms of oceanic carbon sink variability. Chlorophyll is not a direct measurement of biomass and is dependent upon temperature, light, and nutrients [Geider *et al.*, 1998]. Biomass itself is also not a direct measurement of export, as the sinking velocities of particulate matter are dependent upon size. Yet, Lutz *et al.* [2007] show that patterns of biological export do match patterns of productivity, with export occurring nearly simultaneously at low latitudes and lagging production by about 2 months at high latitudes. Do larger peak chlorophyll observations indicate more biomass and export for the entire year? Satellite chlorophyll estimates do not correlate well with simultaneous measurements of oceanic pCO₂ because of differing air-sea gas exchange and remineralization timescales [Lueger *et al.*, 2008], but still years of greater biological productivity might be expected to be years of greater uptake of atmospheric CO₂. Are years of greater daily average chlorophyll years of a greater oceanic carbon sink? What can these satellite estimates of chlorophyll tell us about interannual export variability?

[7] We use an ocean general circulation model coupled to an ecosystem-biogeochemical component to determine whether biology is a first-order control of interannual CO₂ flux variability in the North Atlantic subpolar gyre. We seek to understand how year-to-year variations in biomass affect the annual sink of carbon dioxide in the region and to learn what satellite observations can tell us about a year's anomalous sink. We also consider controls of North Atlantic bloom variability [Follows and Dutkiewicz, 2002; Ueyama and Monger, 2005] and the lack of a significant trend in production in observations in the subpolar North Atlantic [Behrenfeld *et al.*, 2006].

[8] This paper is organized as follows. The next section will describe the model used, experimental setup, and model evaluation. The third section will discuss model results, and the final section includes discussion and conclusions.

2. Model Description

[9] We use a medium-complexity ecosystem model coupled to a three-dimensional North Atlantic regional ocean circulation model.

2.1. Physical Model

[10] We use the MIT general ocean circulation model [Marshall *et al.*, 1997a, 1997b] configured to the bathymetry of the North Atlantic with a horizontal resolution of 0.5° × 0.5°. The model uses a *z* coordinate system of 23 vertical layers. The uppermost layers have finest resolution, with layer depths of 10 m, becoming coarser with depth to 500 m below 2500 m. The Gent-McWilliams [Gent and McWilliams, 1990] eddy parameterization and KPP vertical mixing scheme [Large *et al.*, 1994] simulate effects of sub-grid-scale processes. The bathymetry extends from 20° South to 81.5° North. At the southern boundary, there is a sponge layer in which tracers are rapidly restored to climatology, and the Mediterranean, Labrador and Norwegian Seas have closed boundaries. Temperature and salinity are relaxed to climatology at the

Strait of Gibraltar. Model tracers have a time step of 40 min, and momentum is integrated more rapidly with a time step of 200 s. The physical model is forced with daily winds, heat, freshwater, and radiation data taken from the National Centers for Environmental Prediction (NCEP) Reanalysis I between 1980 and 2006 [Kalnay *et al.*, 1996]. The physical model is spun up for 80 years while relaxing sea surface temperature and salinity to monthly climatology [Boyer *et al.*, 2005] with timescales of 2 weeks and 1 month, respectively. The relaxation forcings during spin up are saved out of the model, and during model experiments discussed here, the relaxations are turned off, but the climatological relaxation forcings are added to interannually varying forcing terms. This increases modeled physical variability.

2.2. Ecosystem Model

[11] The ecosystem model is that of the Dutkiewicz *et al.* [2005] updated to include the cycling of carbon, alkalinity, and oxygen (Figure S1).¹ The model considers the fate of phosphorous, iron, silicon, carbon, and oxygen (results from the latter element are not discussed in this paper) as they pass from dissolved inorganic form to phytoplankton, to zooplankton, and to detritus in both dissolved and sinking particulate forms. Detritus is remineralized back to dissolved inorganic forms. The model includes two phytoplankton functional groups (diatoms and other small phytoplankton) and one zooplankton class. Phytoplankton growth can be limited by multiple nutrients (phosphate, iron, and silicic acid) and light. As an additional update to Dutkiewicz *et al.* [2005] we include temperature dependence on the growth rate following Eppley [1972]. To incorporate this latter change, we have altered the phytoplankton growth rates from those used in Dutkiewicz *et al.* [2005] to 1/1.3 d⁻¹ for small phytoplankton and 1/1.1 d⁻¹ for diatoms. Particulate organic carbon remineralizes at the rate of 1/70 d⁻¹ and sinks at a rate of 8 m d⁻¹. A schematic of the ecosystem model is shown in Figure S1. We refer the reader to Dutkiewicz *et al.* [2005] for further details of the model and parameter selection, and discuss here only the pertinent updates to the model to include the carbon and alkalinity cycle.

[12] Dissolved inorganic carbon (DIC) is taken up by phytoplankton with a fixed C:P ratio of 120 [Anderson and Sarmiento, 1994]. As is done with other nutrients in Dutkiewicz *et al.* [2005], carbon passes through phytoplankton into zooplankton and detrital matter, which in turn remineralizes with constant timescales back to DIC. Additionally, though, carbon is exchanged with the atmosphere. The flux of carbon dioxide between the ocean and atmosphere is parameterized according to Wanninkhof [1992] using daily winds. We define a positive air-sea flux as one directed into the ocean. The pH and DIC in the ocean model surface layers are used to determine the concentration of CO₂ gas and H₂CO₃, which determine oceanic pCO₂. Seawater alkalinity, temperature, salinity, DIC, PO₄, and silicate concentrations determine pH according to Follows *et al.* [2006]. Changes in particulate inorganic carbon (PIC) and nutrient concentrations alter alkalinity following

¹Auxiliary materials are available in the HTML. doi:10.1029/2008GB003241.

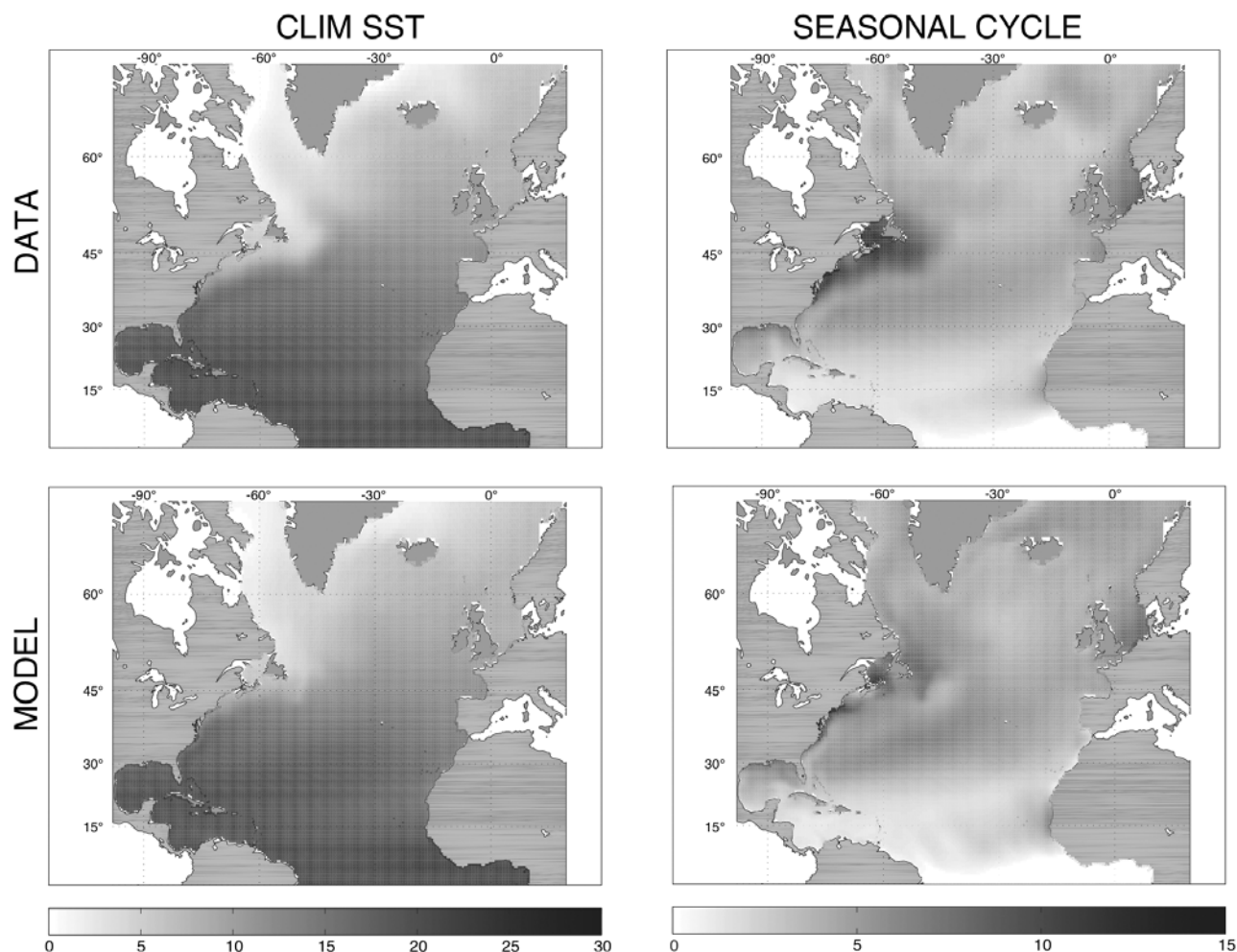


Figure 1. Model and data (Reynolds and Smith reanalysis data provided by the Physical Sciences Division of the Earth System Research Laboratory, Oceanic and Atmospheric Administration, NOAA, Boulder, Colorado, from their Web site at <http://www.cdc.noaa.gov/>) (left) annual average SST and (right) seasonal cycle of SST. Model and data climatology from 1982 to 2006. Seasonal cycle of SST defined as difference between summer/early fall (JAS) mean SST and winter (FMA) mean SST.

OCMIP protocols [Najjar and Orr, 1999]. PIC, representing sinking calcium carbonate shells, is explicitly included, with 7% of phytoplankton assumed to be calcifiers. Dissolution of PIC occurs with a timescale of 360 d^{-1} .

[13] Photosynthetic available radiation (PAR) is assumed to be 40% of the daily NCEP Reanalysis I data 24 h averaged shortwave radiation, a reasonable assumption according to Frouin and Pinker [1995] and Olofsson *et al.* [2007]. Fractional ice coverage is prescribed with daily resolution from NCEP Reanalysis I data, and its presence blocks the same fraction of incoming radiation. The model allows for self-shading as in Dutkiewicz *et al.* [2005]. As also in that paper, phytoplankton biomass ($\mu\text{M P}$) is converted to chlorophyll for diagnostic purposes using the Doney *et al.* [1996] parameterization. We assume that because POC constitutes the majority of carbon removed from the surface ocean, it is also the most important component to interannual variability of export. We neglect the removal of biomass and dissolved carbon by lateral and vertical mixing. For the purpose of this analysis, carbon export is defined to

be the rate of removal of particulate organic carbon through 100 m, as done by Bopp *et al.* [2001]. Export defined in this manner will capture new growth in the photic zone, but the export that does not sink below the depth of the maximum mixed layer may return to the surface ocean during winter mixing.

[14] The biogeochemical model spin up begins in winter and is initialized with GLODAP [Key *et al.*, 2004; Lee *et al.*, 2006] DIC and ALK climatology, World Ocean Atlas 2005 [Garcia *et al.*, 2006a, 2006b] nutrients and oxygen, and very low values of phytoplankton and zooplankton. The ecosystem component is turned on after the 80-year physical model spin up, and the coupled model is spun up for 20 years with a constant atmospheric pCO_2 of 360 ppm. The coupled model is then run for 27 years with daily forcing between 1980 and 2006, and seasonally varying atmospheric pCO_2 increasing according to Mauna Loa observations [Keeling *et al.*, 2001]. The years 1980 and 1981 are ignored in model analysis to allow for adjustment. In order to separate a bloom and the subsequent export from the bloom

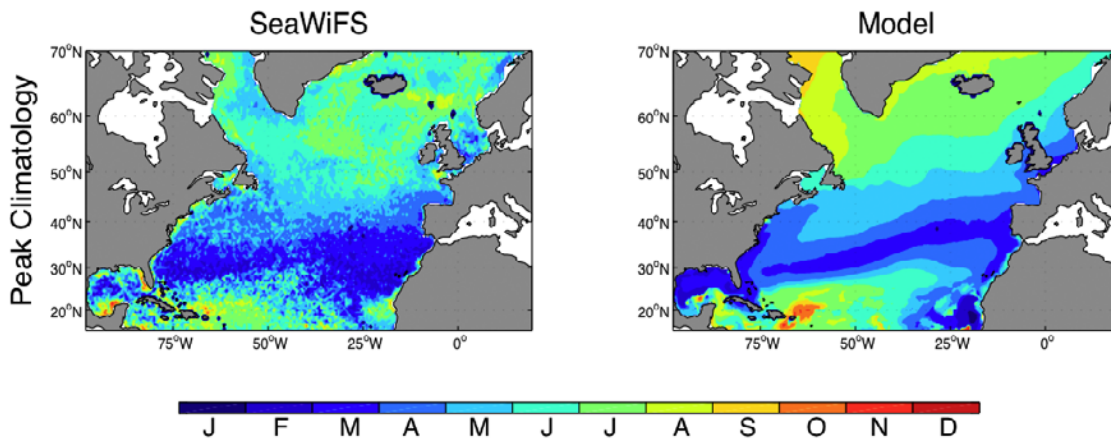


Figure 2. Climatology of bloom peak day in SeaWiFS satellite data (1998–2006) and in the model (1982–2006).

and export of the following year, a year is considered to be 1 December to 30 November for analysis.

2.3. Model-Data Comparisons

[15] The physical model produces realistic surface ocean temperatures which affect pCO₂ and bloom timing. With Figure 1, we show that the physical model adequately

replicates the observed pattern of annual average SST with the exception of a small region off the northeastern coast of North America. The model also captures the amplitude of the seasonal SST cycle. The model produces a realistic pattern of observed interannual SST RMS in the subpolar region, but overestimates this RMS by about 0.25 degrees.

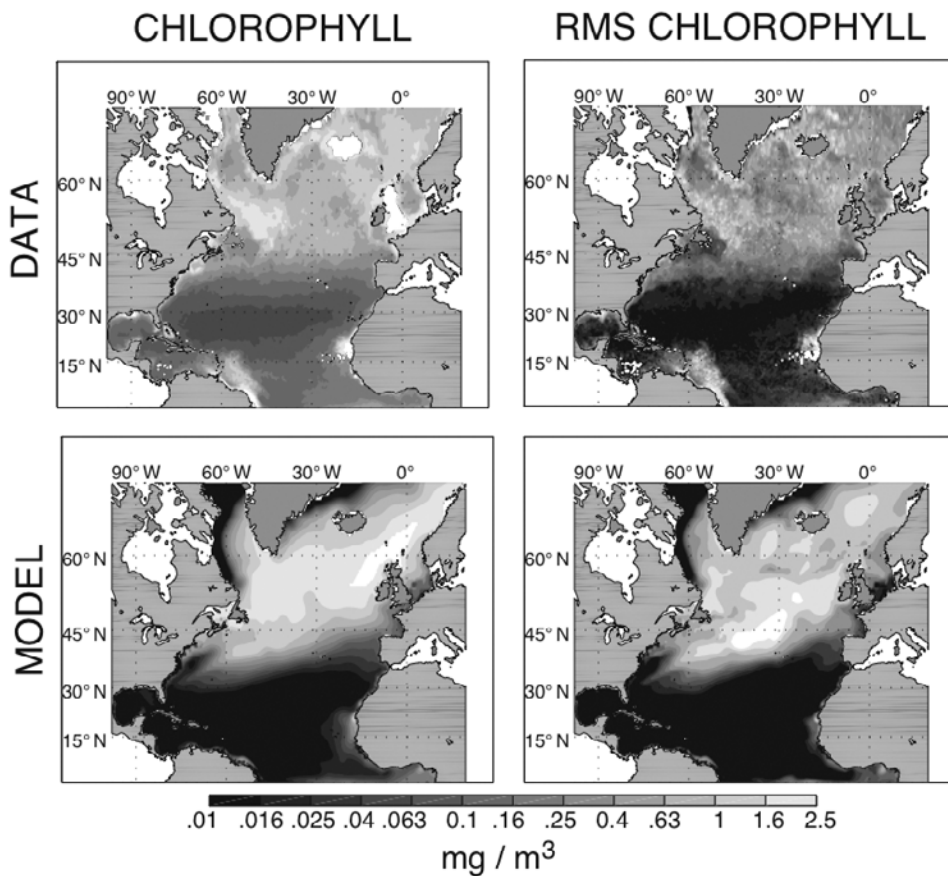


Figure 3. Model surface (55 m) and SeaWiFS climatology and root mean square (RMS) of June chlorophyll mg/m³. Modeled climatology and standard deviation between 1998 and 2006. SeaWiFS data from 1998 to 2006.

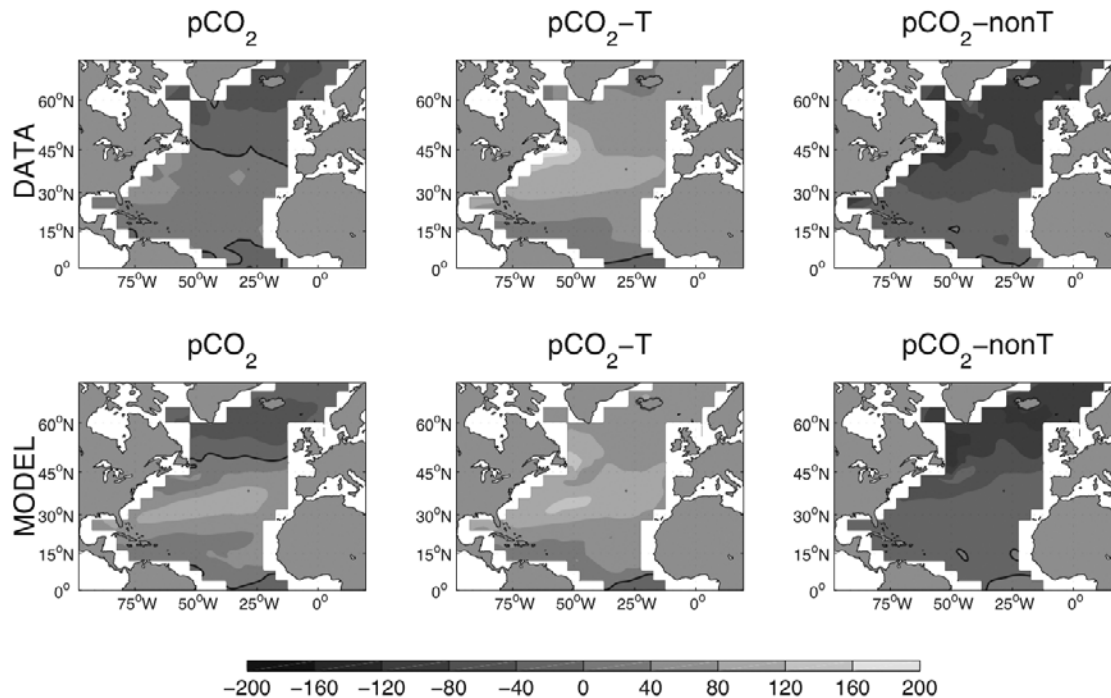


Figure 4. Maps of the seasonal amplitude (ASO – JFM) of $p\text{CO}_2$, $p\text{CO}_2\text{-T}$, and $p\text{CO}_2\text{-nonT}$ in the North Atlantic for the model and observational data of *Takahashi et al.* [2002]. Amplitudes shown are in units of μatm . The dark line is zero seasonal change.

[16] Timing of the bloom is dependent upon both the physical and chemical state of the ocean and may affect the annual biomass and export. For example, blooms that begin later in the subpolar gyre may be limited by the length of the growing season, and those years may have reduced net biomass and export. Timing of modeled bloom peak dates is evaluated using SeaWiFS satellite data from 1998 to 2006. To isolate bloom peak dates, SeaWiFS, 8-day chlorophyll data and daily model chlorophyll were smoothed using a 4-week median filter as in *Ueyama and Monger* [2005], and the peak was defined as the first day between 1 December and 30 November of the maximum chlorophyll value. Figure 2 shows the agreement between the climatological calendar day of peak chlorophyll in the model and satellite data. Bloom start dates (not shown) are determined using the cumulative variance technique as in *Ueyama and Monger* [2005]. We fit a sigmoidal curve to the cumulative variance of the chlorophyll time series in each model grid cell. The start of the bloom is determined as the first day the slope of the curve reaches twenty percent of its maximum value. We find that the bloom begins in the fall in the lower latitudes and progresses northward through the spring and summer, similar to that found by *Ueyama and Monger* [2005].

[17] The climatology of modeled and observed chlorophyll and standard deviation of chlorophyll during the subpolar bloom peak in the model and 8 years of observations are shown in Figure 3. The depth to which SeaWiFS is retrieving ocean color varies in both space and time. For the model, the surface chlorophyll concentration is considered to be the mean value in the top 55 m. Results and patterns

are robust with differing selections of the depth to which model chlorophyll is averaged. The model replicates the pattern and cycle of observed chlorophyll well, but overestimates the magnitude of peak chlorophyll in the subpolar region by a factor of two to three. The model underestimates chlorophyll in the subtropical region, a problem common in models that do not explicitly model eddies [*McGillicuddy et al.*, 2007; *Oschlies and Garçon*, 1998]. One additional potential reason for our underestimation of chlorophyll is that we neglect nitrogen fixation. However, satellite retrieval of surface chlorophyll does have an error on the order of 30% globally [*Gregg and Casey*, 2004].

[18] Surface ocean $p\text{CO}_2$ is affected by temperature (SST), alkalinity (ALK), salinity (SSS), and dissolved inorganic carbon (DIC). In order to understand how biology affects the $p\text{CO}_2$, we separate the temperature-driven $p\text{CO}_2$ ($p\text{CO}_2\text{-T}$) from the effects of alkalinity, salinity, and DIC ($p\text{CO}_2\text{-nonT}$) according to the equations of *Takahashi et al.* [2002], on the basis of experimental results of *Takahashi et al.* [1993]. This separation is valuable in the study of the subpolar North Atlantic because DIC and temperature are the two dominating controls on $p\text{CO}_2$ in the region [*Ullman et al.*, 2009]. The $p\text{CO}_2\text{-nonT}$ can be understood primarily as the effect of DIC.

$$p\text{CO}_2 - T = \overline{p\text{CO}_2} \times \exp(0.0423 \times (\overline{SST} - SST)) \quad (1)$$

$$p\text{CO}_2 - \text{nonT} = p\text{CO}_2 \times \exp(0.0423 \times (\overline{SST} - SST)) \quad (2)$$

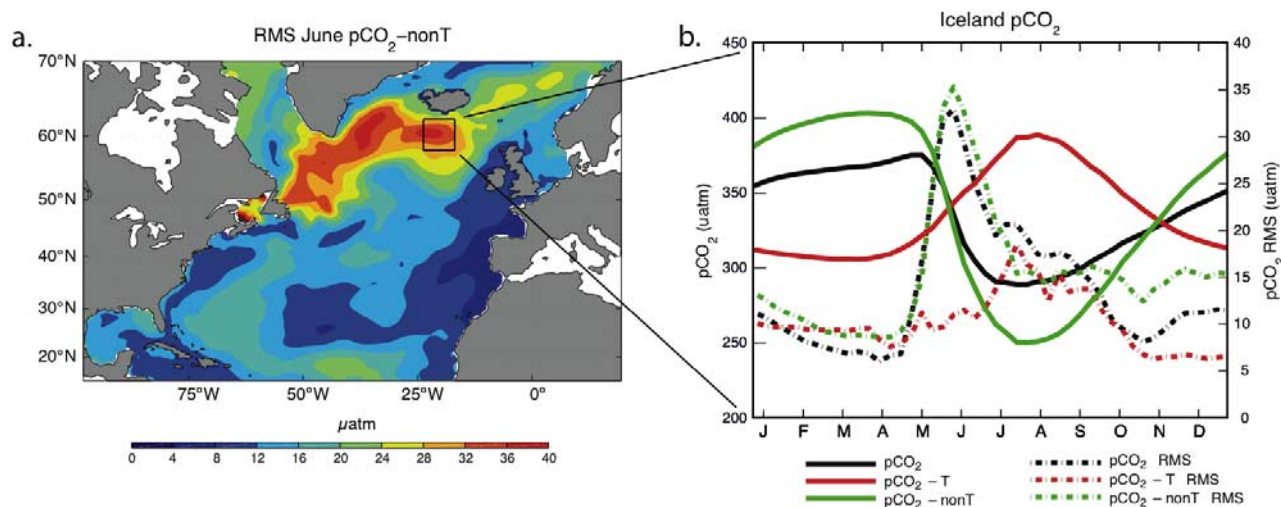


Figure 5. (a) Standard deviation of 25 years of June $p\text{CO}_2\text{-nonT}$ in μatm . The large variability in June $p\text{CO}_2$ (not shown) in the subpolar region is due to $p\text{CO}_2\text{-nonT}$ variability. The boxed region corresponds to the Icelandic region depicted in Figure 5b. (b) Twenty-five year climatology of the $p\text{CO}_2$ seasonal cycle and root mean square of weekly $p\text{CO}_2$ and each of its components near Iceland (57.5°N 17.5°W). Summertime variability in $p\text{CO}_2$ is driven by variability in $p\text{CO}_2\text{-nonT}$.

The bar represents a time averaged mean value. Although the equations are not linear, when separating daily model output $p\text{CO}_2$, the temperature and nontemperature components sum to within a couple μatm of total $p\text{CO}_2$.

[19] We can compare these components of the model's carbon cycle to observations. In Figure 4, the seasonal cycle of total $p\text{CO}_2$ and each of the $p\text{CO}_2$ components are shown compared to the climatology of *Takahashi et al.* [2002]. The seasonal cycle is defined as the mean over the late summer/early fall months (August, September, October) minus the 3-month winter mean (January, February, March). The model does well capturing the observed pattern of the seasonal cycle of $p\text{CO}_2$, clearly illustrating the dominance of temperature to the cycle in the subtropics and the dominance of DIC cycling in the subpolar region. The cycle of $p\text{CO}_2\text{-nonT}$ is slightly stronger than observed in the subpolar region because of the large model bloom there. The weak bloom in the subtropical region causes a weaker seasonal cycle of $p\text{CO}_2\text{-nonT}$ than observed. The seasonal cycle of $p\text{CO}_2\text{-T}$ is a bit strong at subtropical locations.

[20] In summary, the coupled model does a good job capturing the timing and pattern of the spring bloom and the seasonal cycle of SSTs and $p\text{CO}_2$ throughout much of the North Atlantic basin. The primary deficiency is that mean chlorophyll is too low in the subtropical region. Despite this, patterns of variability in chlorophyll (Figure 3) are consistent with data across the basin, and thus we conclude the model is an adequate tool for understanding the effect of biological variability on air-sea CO_2 fluxes.

3. Results

3.1. Bloom Timing and $p\text{CO}_2$

[21] We would like to understand whether interannual variations in the magnitude of the North Atlantic spring bloom have an effect on yearly export and CO_2 fluxes. In

Figure 5a, we show the standard deviation of 25 years of monthly averaged June $p\text{CO}_2\text{-nonT}$ from the model. The subpolar region shows large variability in the magnitude of June $p\text{CO}_2$ during the height of the bloom because of interannual variability in DIC changes from biological activity. Zooming in on the boxed region near Iceland shown in Figure 5a, we show the seasonal cycle of weekly $p\text{CO}_2$ and its standard deviation (black dashed) in Figure 5b. The largest variability in total $p\text{CO}_2$ occurs during June and is due to changes in the $p\text{CO}_2\text{-nonT}$ component, that is, in turn, due to bloom timing and magnitude variability. This maximum in variability occurs during the time of maximum change in the seasonal cycle of total $p\text{CO}_2$. This suggests that variability in the bloom timing might impact yearly CO_2 fluxes.

[22] The importance of the bloom to the seasonal cycle of $p\text{CO}_2$ is shown in Figure 6a, where significant positive correlations between the bloom peak date and the date of minimum oceanic $p\text{CO}_2$ are shown. Positive correlations north of 45°N indicate that bloom timing affects the date of the annual minimum $p\text{CO}_2$. Earlier blooms shift this minimum earlier, and later blooms shift the minimum $p\text{CO}_2$ later. The correlation between 30°N and 45°N is surprising, because temperature controls $p\text{CO}_2$ in this region. Here, minimum $p\text{CO}_2$ occurs when the water is coldest and mixing most vigorously. Chlorophyll peaks at the same time, because the mixing supplies nutrients, and at the same time DIC (Figure 6b) to the surface, but it is the cold that causes the $p\text{CO}_2$ minimum, not biology.

3.2. Export and CO_2 Fluxes

[23] Ocean biology controls summertime $p\text{CO}_2$ in the subpolar region, but does this summertime control of $p\text{CO}_2$ exert a first-order control on the annual CO_2 fluxes in the region? SeaWiFS provides satellite-derived estimates of year-to-year variations in ocean chlorophyll. It is

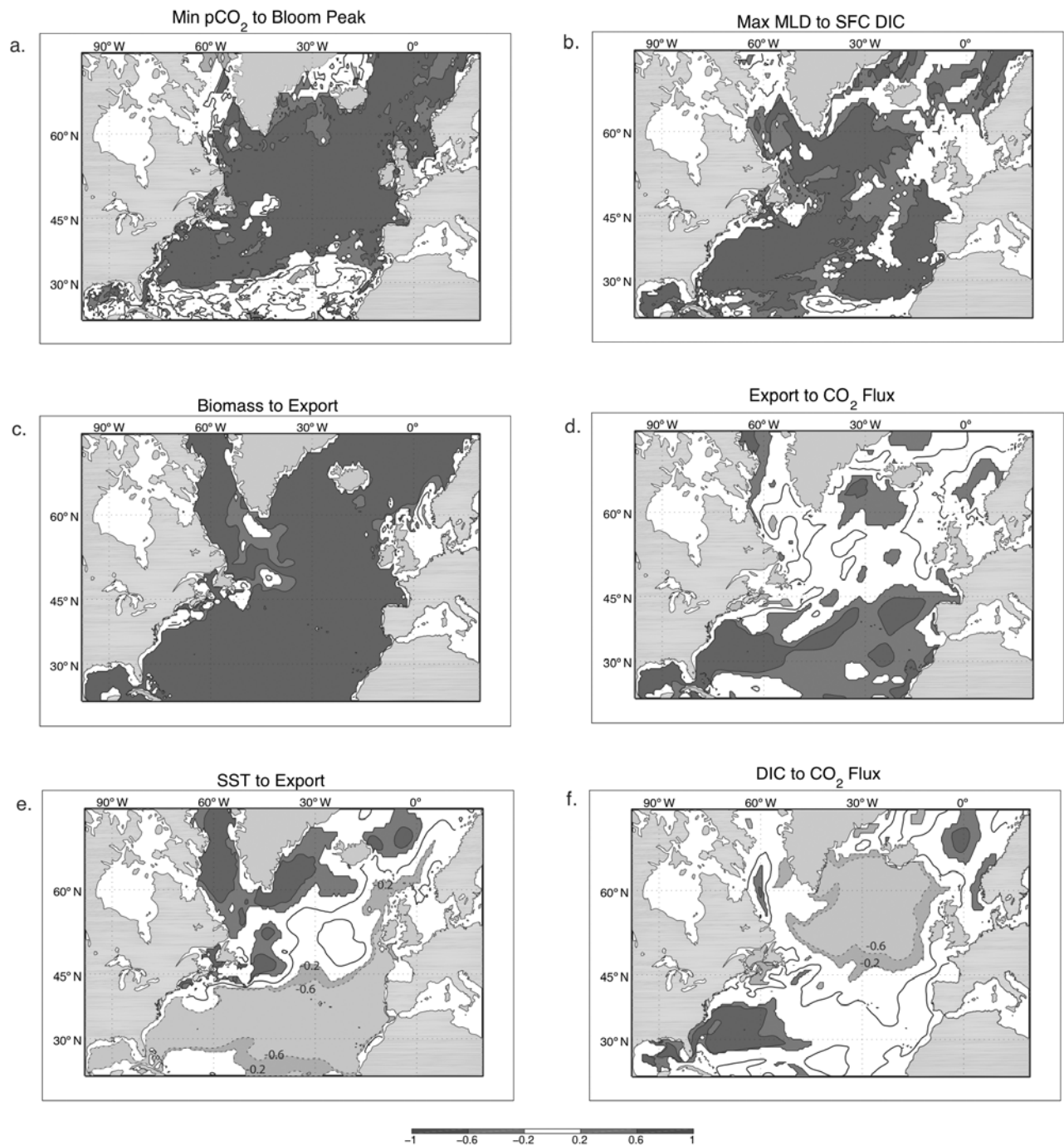


Figure 6. (a) Significant correlations between the day of the year of the bloom peak and the day of the year of the minimum oceanic pCO₂ value. (b) Significant correlations between the annual maximum mixed layer depth and surface DIC concentrations. (c) Significant correlations between annual biomass and annual export. (d) Significant correlations between annual export and detrended annual air-sea CO₂ flux. (e) Significant correlations between annual average SST and annual export. (f) Significant correlations between annual surface DIC concentrations and the annual air-sea CO₂ flux. All correlations presented take into account the temporal autocorrelation between the two time series as in the work of *Bretherton et al.* [1999] and are considered significant at the 95% confidence level. Dashed and labeled contour lines indicate a negative correlation. The thick black lines are lines of zero correlation.

expected that years with larger chlorophyll peaks and annually integrated chlorophyll are years of greater export of particulate organic carbon, even though chlorophyll is not a direct measurement of biomass. We test this expectation.

[24] The correlation between modeled integrated annual biomass in the top 55 m (December–November) and integrated export over the same time period is significantly correlated almost everywhere in the North Atlantic (Figure 6c). Thus, greater biological productivity does result in more export, but do larger blooms create an anomalous influx of CO₂ for the year? We consider this by correlating the annual CO₂ flux (positive into ocean) and annual export (Figure 6d). Large-scale correlation between annual CO₂ fluxes and annual export exists in the subtropical region, but not in the majority of the subpolar region.

[25] As with the seasonal cycle (section 3.1), the large-scale correlation between annual CO₂ fluxes and annual export in the subtropical region does not indicate a first-order control of biology in that region; instead it indicates an indirect relationship via temperature. Years of increased mixing bring both cold and nutrient rich waters to the surface. Increased nutrient supply fuels increased biomass growth and export in this nutrient limited region. However, oceanic pCO₂ in the subtropical North Atlantic is largely controlled by temperature [Lueger *et al.*, 2008; Ullman *et al.*, 2009], and it is the anomalously cold temperatures that lead to a reduced pCO₂. Colder years are therefore years of greater biological production and (indirectly) lower pCO₂ in the region, in agreement with the findings of Bopp *et al.* [2001] and Sarmiento *et al.* [2004]. Annual temperatures and maximum winter mixed layer depth, as defined as the depth at which the potential density differs from the surface by 0.125 kg/m³, are significantly anticorrelated almost everywhere (not shown).

[26] Thus, we find that years of greater biological production in the subpolar region are years of greater export, but not necessarily years of a greater influx of CO₂. In the western subpolar region, where light is seasonally limiting, export is positively correlated to annual SST (Figure 6e), indicating that warmer years and years of greater stratification provide more light and less bloomtime mixing, and thus greater biological productivity [Follows and Dutkiewicz, 2002; Ueyama and Monger, 2005]. These are also years of a reduced supply of DIC to the surface. Figure 6f illustrates that the air-sea CO₂ flux is inversely proportional to DIC in the high latitudes. Years of lower surface DIC are years of increased CO₂ influx in this region, but is the lower DIC due to shallower winter mixing or greater biological drawdown? Using the model, we are able to quantify the change in DIC created by biological production above or below the 25-year daily mean (Text S1). We find the day-to-day change in pCO₂ above or below its mean value due to biological activity amounts to a daily average change in pCO₂ on the order of 2 μatm or less in the subpolar gyre during summer, consistent with Le Quéré *et al.* [2003], who used a model sensitivity test to determine that biological interannual variability only altered pCO₂ by a couple of μatm. Changes in pCO₂ caused by anomalous winter mixing in the model are larger than those caused by anomalous biological productivity (on the order of 10 μatm,

Text S1). Increased wind speeds in winter also cause increased air-sea gas exchange, so winter mixing must be controlling the annual CO₂ flux variability. These factors combine such that winter flux variability is significantly larger than summer flux variability in the subpolar gyre (Figure S2).

[27] The small area within the subpolar gyre to the southwest of Iceland that shows a significant correlation between export and CO₂ flux variability (Figure 6d) is a region of extremely deep winter mixing. In this region, anomalous biological production is not a first-order control of air-sea flux variability, but mixing is highly correlated to biomass here. Deeper mixing in this region increases surface DIC concentrations and decreases the magnitude of the spring bloom by keeping phytoplankton mixed away from the light [Dutkiewicz *et al.*, 2001]. In this way, years of decreased mixing are also years of both increased air-sea CO₂ flux and increased export in this small region, but the correlation is indirect.

[28] Across the basin, years of increased integrated chlorophyll are indeed years of greater export, but years of greater export are not necessarily years of an increased air-sea CO₂ uptake. Export and CO₂ fluxes are correlated in the subtropics, but it is temperature, not biology, that controls pCO₂ in this region, so the correlation is indirect. In the subpolar region, anomalies in export do not correlate with air-sea CO₂ flux anomalies. We find that biology is not a first-order control on interannual air-sea CO₂ flux variability anywhere in the North Atlantic.

3.3. Biological Variability

[29] We have shown that biological productivity in the subpolar region determines the seasonal cycle of pCO₂ (Figure 3, 5), so why is it not a first-order control of air-sea CO₂ flux variability (Figure 6d)? DIC controls the annual pCO₂ and air-sea CO₂ fluxes in the subpolar region, but anomalous summertime biomass does not create anomalous annual CO₂ fluxes (Figure 6d, 6f). In this section, we illustrate that large variability in June pCO₂ (Figure 5) is driven by bloom timing, not integrated magnitude of the bloom. For our analysis, we define integrated bloom strength as the annually integrated chlorophyll.

[30] The ratio of the standard deviation in daily chlorophyll to the mean between 1998 and 2006 is shown for the model and SeaWiFS in Figure 7a, 7b. Since the model is unable to produce the magnitude of the bloom observed in the subtropical region (Section 2.3), percent variations in less productive regions are unrealistically large, and so areas in which the model integrated annual average chlorophyll is less than 150 mg m⁻³ are masked. We consider only the variability in the subpolar North Atlantic. The model does very well at capturing the percent of biological variability throughout the subpolar region, even capturing specific regions of observed greater variability, such as along 30°W. For the area shown in Figure 7a, 7b, the average percent variability is 13.5% in the data and 15.3% in the model. This percent variability agrees reasonably well with Lévy *et al.* [2005] who find annually integrated chlorophyll varies by 10% of its mean in a region of the subpolar North Atlantic (16–22°W, 41–50°N) using SeaWiFS satellite estimates of chlorophyll for 1998–2002.

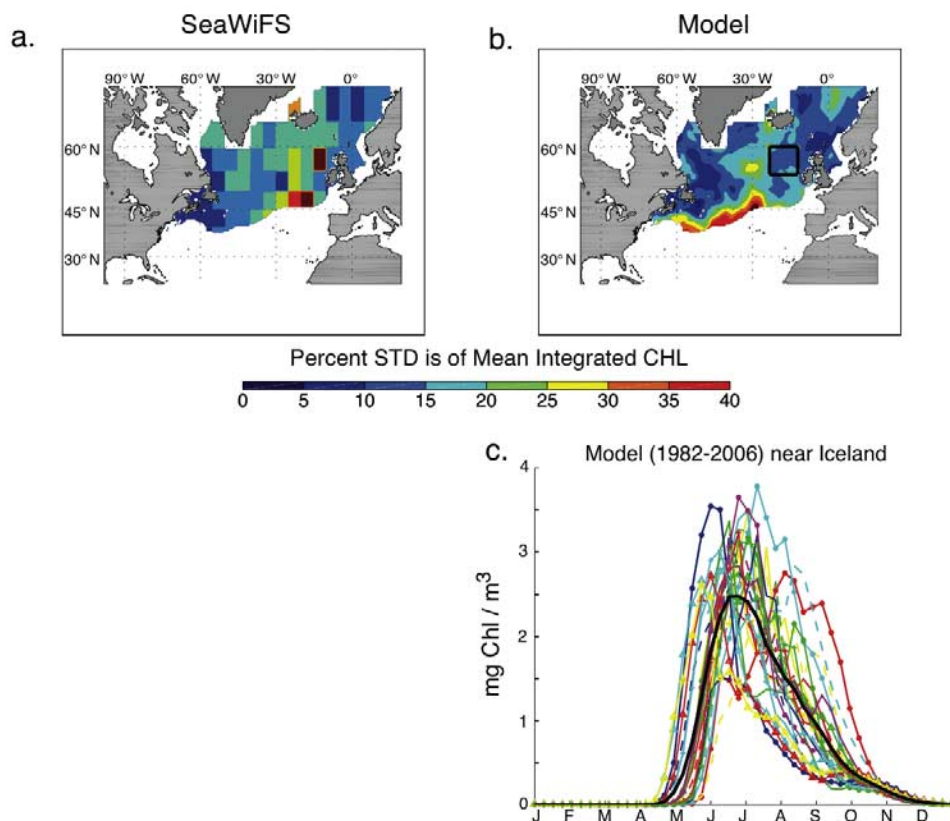


Figure 7. (a, b) The percent the standard deviation is of the mean daily chlorophyll between fall 1998 and 2006 in (Figure 7a) SeaWiFS and (Figure 7b) the model. Eight-day weeks 10 through 37 of the year are used in this analysis, because SeaWiFS data in the subpolar region is too sparse during the omitted weeks. To compare the model to SeaWiFS satellite data, a daily average chlorophyll value for each year was calculated in both the data and model. Because of cloud cover and other satellite issues, not all grid points have observational data every 8-day period, so area-weighted averages for $5^{\circ} \times 5^{\circ}$ regions were used with observational data. Within a $5^{\circ} \times 5^{\circ}$ area, the available data for each 8-day record is assumed representative of the entire area and an area-weighted average is created, ignoring missing data points. The model is able to capture the percent variability observed and much of the pattern of variability magnitude. (c) Twenty-five years of modeled chlorophyll at region near Iceland boxed in Figure 7b. Thick black line is modeled climatology. Annually integrated chlorophyll varies by only 10.9% of the mean, and annual export varies by only 4.8% of the mean between 1982 and 2006. SeaWiFS daily average chlorophyll (1998–2006) varies by 18% of its mean in this region.

[31] The box in Figure 7b corresponds to the near-Iceland region introduced in Figure 5, and Figure 7c depicts the 25 years of model chlorophyll in that region. Though large year-to-year variations in bloom timing exist, the variability in integrated bloom strength (the area underneath each curve) and export are small. This indicates that variations in bloom timing drive a large variability in June pCO₂ (Figure 5) but do not translate into significant anomalies in integrated chlorophyll or export over the course of the year. The percent variation of modeled annual export in this near-Iceland region (4.8%) is much less than the percent variation in modeled yearly chlorophyll (10.9%), since chlorophyll is not a direct measurement of biomass and does not take into account changing community structure. Its variability does not translate to export variability. Between 1998 and 2006, integrated chlorophyll varied by 18% of its mean in SeaWiFS data at this location.

[32] In the subpolar gyre of the North Atlantic, we find that blooms that start earlier also end earlier, an unexpected result for a light-limited region. Further model analysis indicates that tight ecosystem coupling is responsible for limiting interannual variability of integrated bloom strength. An initial diatom bloom begins to reduce silicate and phosphorous availability. At the same time, zooplankton concentrations increase. When silicate is limited, the diatom bloom subsides and small phytoplankton begin to dominate the biomass. When nutrients limit growth, the phytoplankton concentrations decrease. Mixing in late fall relaxes nutrient limitation, but zooplankton are too abundant to allow another bloom. This progression was observed by *Sieracki et al.* [1993] and discussed by *Lochte et al.* [1993] during the North Atlantic Bloom Experiment.

[33] With limited variability in integrated bloom magnitude, there is limited variability in the annual strength of the

biological pump. This variability in the biological pump is too weak to be a first-order control on the air-sea CO₂ flux variability in the region.

4. Discussion and Conclusions

[34] We have used a basin-scale ocean general circulation model coupled to a medium complexity ecosystem to determine whether variation in biological productivity is a first-order control on air-sea CO₂ fluxes in the subpolar North Atlantic. We have shown that large variability in summer pCO₂ exists in the subpolar region and is due to the bloom's control on the seasonal cycle of pCO₂. However, upon closer inspection, the large variability present in summer is due to bloom timing and not integrated bloom strength. Although no significant causal relationship was found between variations in subpolar biomass and annual subpolar CO₂ fluxes, biology does determine the timing of the seasonal cycle of pCO₂ within the region and is an important driver of the mean air-sea gas exchange [Behrenfeld *et al.*, 2006; Laws *et al.*, 2000]. The pattern of annual mean CO₂ fluxes matches the pattern of annual export (Figure S3), illustrating the importance of biology to the mean air-sea gas exchange.

[35] The model replicates the percent chlorophyll variability observed in SeaWiFS in the subpolar gyre, and the small percent variability in modeled annually integrated export (5–10%) suggests that it is not sufficient to be a first-order control of annual CO₂ flux variability. Modeled biological variability alters summertime daily average pCO₂ on the order of a couple μatm . Light summer winds over the subpolar gyre further also help to limit biological impacts on air-sea CO₂ flux variability.

[36] In the subtropical region, yearly biological production and export are significantly correlated to annual CO₂ fluxes, but the relationship is not causal. Here, SST controls pCO₂ but is related to biology through the vertical supply of nutrients. Colder SSTs decrease oceanic pCO₂, increase vertical mixing, and enhance the bloom. Our results agree with Behrenfeld *et al.* [2006] who find a strong correlation between biological production and climate within the permanently stratified regions of the ocean. However, we do not anticipate any effect on the CO₂ fluxes due to the changes in biological production. Even though modeled biological variability in the subtropical region exceeds 100 percent, it is still not a first-order control of pCO₂, because SST controls pCO₂ here [Ullman *et al.*, 2009]. Therefore, we conclude that biology has not been a first-order control on the interannual variability of CO₂ fluxes anywhere in the North Atlantic in recent years, barring changes in ecosystem structure that would not be captured in this model.

[37] Despite biology not controlling CO₂ flux interannual variability, interpretation of in situ observations of oceanic pCO₂ need to carefully consider bloom timing in order to properly understand CO₂ cycling, variability, and trends. Model results show that changes in bloom timing can alter monthly pCO₂ values by tens of μatm (Figure 5), so sparse observations should be extrapolated to annual timescales with great care.

[38] Recent studies have used SeaWiFS data to understand year-to-year variations and trends in biological productivity on a global scale. Our results suggest SeaWiFS may be very useful for estimating variability in export out of the ocean surface on short timescales, but cannot directly elucidate CO₂ flux variability on annual timescales.

[39] **Acknowledgments.** We thank Dierk Polzin for assistance with the figures and the computations, Mick Follows for advice, and two anonymous reviewers for their helpful suggestions. We thank NASA for funding (CARBON/04-0300-0228). Ocean color data used in this study were produced by the SeaWiFS Project at GSFC. The data were obtained from the GESDAAC under the auspices of the NASA. Use of this data is in accord with the SeaWiFS Research Data Use Terms and Conditions Agreement. Reynolds and Smith reanalysis data provided by the Physical Sciences Division of the Earth System Research Laboratory, Oceanic and Atmospheric Administration, NOAA, Boulder, Colorado, from their Web site at <http://www.edc.noaa.gov/>.

References

- Anderson, L. A., and J. L. Sarmiento (1994), Redfield ratios of remineralization determined by nutrient data analysis, *Global Biogeochem. Cycles*, 8(1), 65–80, doi:10.1029/93GB03318.
- Behrenfeld, M. J., R. T. O'Malley, D. A. Siegel, C. R. McClain, J. L. Sarmiento, G. C. Feldman, A. J. Milligan, P. G. Falkowski, R. M. Letelier, and E. S. Boss (2006), Climate-driven trends in contemporary ocean productivity, *Nature*, 444, 752–755, doi:10.1038/nature05317.
- Bopp, L., P. Monfray, O. Aumont, J.-L. Dufresne, H. Le Treut, G. Madec, L. Terray, and J. Orr (2001), Potential impact of climate change on marine export production, *Global Biogeochem. Cycles*, 15(1), 81–99, doi:10.1029/1999GB001256.
- Boyer, T. P., S. Levitus, H. E. Garcia, R. A. Locarnini, C. Stephens, and J. Antonov (2005), Objective analyses of annual, seasonal, and monthly temperature and salinity for the world ocean on a 0.25 degrees grid, *Int. J. Climatol.*, 25(7), 931–945, doi:10.1002/joc.1173.
- Bretherton, C. S., M. Widmann, V. P. Dymnikov, J. M. Wallace, and I. Bladé (1999), The effective number of spatial degrees of freedom of a time-varying field, *J. Clim.*, 12, 1990–2009, doi:10.1175/1520-0442(1999)012<1990:TENOSD>2.0.CO;2.
- Canadell, J. G., C. Le Quére, M. R. Raupach, C. B. Field, E. T. Buitenhuis, P. Ciais, T. J. Conway, N. P. Gillett, R. A. Houghton, and G. Marland (2007), Contributions to accelerating atmospheric CO₂ growth from economic activity, carbon intensity, and efficiency of natural sinks, *Proc. Natl. Acad. Sci. U. S. A.*, 104(47), 18,866–18,870.
- Doney, S., D. M. Glover, and R. G. Najjar (1996), A new coupled, one-dimensional biological-physical model for the upper ocean: Applications to the JGOFS Bermuda Atlantic Time-Series Study (BATS) site, *Deep Sea Res., Part II*, 43(2–3), 591–624, doi:10.1016/0967-0645(95)00104-2.
- Dutkiewicz, S., M. Follows, J. Marshall, and W. W. Gregg (2001), Interannual variability of phytoplankton abundances in the North Atlantic, *Deep Sea Res., Part II*, 48(10), 2323–2344, doi:10.1016/S0967-0645(00)00178-8.
- Dutkiewicz, S., M. J. Follows, and P. Parekh (2005), Interactions of the iron and phosphorus cycles: A three-dimensional model study, *Global Biogeochem. Cycles*, 19, GB1021, doi:10.1029/2004GB002342.
- Eppley, R. W. (1972), Temperature and phytoplankton growth in the sea, *Fish. Bull.*, 70, 1063–1085.
- Follows, M., and S. Dutkiewicz (2002), Meteorological modulation of the North Atlantic spring bloom, *Deep Sea Res., Part II*, 49(1–3), 321–344, doi:10.1016/S0967-0645(01)00105-9.
- Follows, M., T. Ito, and S. Dutkiewicz (2006), A compact and accurate carbonate chemistry solver for ocean biogeochemistry models, *Ocean Modell.*, 12, 290–301, doi:10.1016/j.ocemod.2005.05.004.
- Frouin, R., and R. T. Pinker (1995), Estimating photosynthetically active radiation (PAR) at the Earth's surface from satellite observations, *Remote Sens. Environ.*, 51, 98–107, doi:10.1016/0034-4257(94)00068-X.
- Garcia, H. E., R. A. Locarnini, T. P. Boyer, and J. I. Antonov (2006a), *World Ocean Atlas 2005*, vol. 4, *Nutrients (Phosphate, Nitrate, Silicate)*, *NOAA Atlas NESDIS 64*, edited by S. Levitus, 396 pp., U.S. Govt. Print. Off., Washington, D. C.
- Garcia, H. E., R. A. Locarnini, T. P. Boyer, and J. I. Antonov (2006b), *World Ocean Atlas 2005*, vol. 3, *Dissolved Oxygen, Apparent Oxygen Utilization, and Oxygen Saturation*, *NOAA Atlas NESDIS 63*, edited by S. Levitus, U.S. Govt. Print. Off., 342 pp., Washington, D. C.

- Geider, R. J., H. L. MacIntyre, and T. M. Kana (1998), A dynamic regulatory model of phytoplankton acclimation to light, nutrients, and temperature, *Limnol. Oceanogr.*, *43*(4), 679–694.
- Gent, P. R., and J. C. McWilliams (1990), Isopycnal mixing in ocean circulation models, *J. Phys. Oceanogr.*, *20*, 150–155, doi:10.1175/1520-0485(1990)020<0150:IMIOC>2.0.CO;2.
- Gregg, W. W., and N. Casey (2004), Global and regional evaluation of the SeaWiFS chlorophyll data set, *Remote Sens. Environ.*, *93*, 463–479, doi:10.1016/j.rse.2003.12.012.
- Kalnay, E., et al. (1996), The NCEP/NCAR 40-Year Reanalysis Project, *Bull. Am. Meteorol. Soc.*, *77*(3), 437–471, doi:10.1175/1520-0477(1996)077<0437:TNYRP>2.0.CO;2.
- Keeling, C. D., S. C. Piper, R. B. Bacastow, M. Wahlen, T. P. Whorf, M. Heimann, and H. A. Meijer (2001), *Exchanges of Atmospheric CO₂ and ¹³CO₂ With the Terrestrial Biosphere and Oceans From 1978 to 2000: I. Global Aspects*, *SIO Ref. Ser. 01-06*, 88 pp., Scripps Inst. of Oceanogr., San Diego, Calif.
- Key, R. M., A. Kozyr, C. L. Sabine, K. Lee, R. Wanninkhof, J. Bullister, R. A. Feely, F. Millero, C. Mordy, and T.-H. Peng (2004), A global ocean carbon climatology: Results from GLODAP, *Global Biogeochem. Cycles*, *18*, GB4031, doi:10.1029/2004GB002247.
- Large, W. G., J. C. McWilliams, and S. C. Doney (1994), Oceanic vertical mixing: A review and a model with a nonlocal boundary layer parameterization, *Rev. Geophys.*, *32*, 363–403, doi:10.1029/94RG01872.
- Laws, E. A., P. G. Falkowski, W. O. Smith Jr., H. Ducklow, and J. J. McCarthy (2000), Temperature effects on export production in the open ocean, *Global Biogeochem. Cycles*, *14*(4), 1231–1246, doi:10.1029/1999GB001229.
- Lee, K., L. T. Tong, F. J. Millero, C. L. Sabine, A. G. Dickson, C. Goyet, G.-H. Park, R. Wanninkhof, R. A. Feely, and R. M. Key (2006), Global relationships of total alkalinity with salinity and temperature in surface waters of the world's oceans, *Geophys. Res. Lett.*, *33*, L19605, doi:10.1029/2006GL027207.
- Le Quéré, C., O. Aumont, P. Monfray, and J. Orr (2003), Propagation of climatic events on ocean stratification, marine biology, and CO₂: Case studies over the 1979–1999 period, *J. Geophys. Res.*, *108*(C12), 3375, doi:10.1029/2001JC000920.
- Lévy, M., Y. Lehn, J.-M. André, L. Mémery, H. Loisel, and E. Heifetz (2005), Production regimes in the Northeast Atlantic: A study based on SeaWiFS chlorophyll and OGCM mixed-layer depth, *J. Geophys. Res.*, *110*, C07S10, doi:10.1029/2004JC002771.
- Lochte, K., H. W. Ducklow, M. J. R. Fasham, and C. Stienen (1993), Plankton succession and carbon cycling at 47°N 20°W during the JGOFS North Atlantic Bloom Experiment, *Deep Sea Res., Part II*, *40*(1), 91–114, doi:10.1016/0967-0645(93)90008-B.
- Lueger, H., R. Wanninkhof, A. Olsen, J. Triñanes, T. Johannessen, D. W. R. Wallace, and A. Körtzinger (2008), *The Sea-Air CO₂ Flux in the North Atlantic Estimated From Satellite and ARGO Profiling Float Data*, *NOAA Tech. Memo. OAR AOML-96*, 28 pp., Atl. Oceanogr. and Meteorol. Lab., NOAA, Miami, Fla.
- Lutz, M. J., K. Caldeira, R. B. Dunbar, and M. Behrenfeld (2007), Seasonal rhythms of net primary production and particulate organic carbon flux to depth describe the efficiency of biological pump in the global ocean, *J. Geophys. Res.*, *112*, C10011, doi:10.1029/2006JC003706.
- Marshall, J., A. Adcroft, C. Hill, L. Perelman, and C. Heisey (1997a), A finite volume, incompressible Navier-Stokes model for studies of the ocean on parallel computers, *J. Geophys. Res.*, *102*, 5753–5766, doi:10.1029/96JC02775.
- Marshall, J., C. Hill, L. Perelman, and A. Adcroft (1997b), Hydrostatic, quasi-hydrostatic, and nonhydrostatic ocean modeling, *J. Geophys. Res.*, *102*, 5733–5752, doi:10.1029/96JC02776.
- McGillicuddy, D., et al. (2007), Eddy/wind interactions stimulate extraordinary mid-ocean plankton blooms, *Science*, *316*(5827), 1021–1026, doi:10.1126/science.1136256.
- Najjar, R. G., and J. C. Orr (1999), Biotic-HOWTO, internal OCMIP report, 15 pp., LSCE/CEA Saclay, Gif-sur-Yvette, France.
- Olofsson, P., P. E. Van Laake, and L. Eklundh (2007), Estimation of absorbed PAR across Scandinavia from satellite measurements. Part I: Incident PAR, *Remote Sens. Environ.*, *110*, 252–261, doi:10.1016/j.rse.2007.02.021.
- Oschlies, A., and V. Garçon (1998), Eddy-induced enhancement of primary production in a model of the North Atlantic Ocean, *Nature*, *394*, 266–269, doi:10.1038/28373.
- Raupach, M., G. Marland, P. Ciais, C. Le Quéré, J. Canadell, G. Klepper, and C. B. Field (2007), Global and regional drivers of accelerating CO₂ emissions, *Proc. Natl. Acad. Sci. U. S. A.*, *104*(24), 10,288–10,293, doi:10.1073/pnas.0700609104.
- Sabine, C. L., et al. (2004), The oceanic sink for anthropogenic CO₂, *Science*, *305*, 367, doi:10.1126/science.1097403.
- Sarmiento, J. L., and T. M. C. Hughes (1999), Keynote perspective: Anthropogenic CO₂ uptake in a warming ocean, *Tellus, Ser. B*, *51*(2), 560–561.
- Sarmiento, J. L., et al. (2004), Response of ocean ecosystems to climate warming, *Global Biogeochem. Cycles*, *18*, GB3003, doi:10.1029/2003GB002134.
- Schuster, U., and A. J. Watson (2007), A variable and decreasing sink for atmospheric CO₂ in the North Atlantic, *J. Geophys. Res.*, *112*, C11006, doi:10.1029/2006JC003941.
- Sieracki, M., P. Verity, and D. Stoecker (1993), Plankton community response to sequential silicate and nitrate depletion during the 1989 North Atlantic spring bloom, *Deep Sea Res., Part II*, *40*(1), 213–225, doi:10.1016/0967-0645(93)90014-E.
- Takahashi, T., J. Olafsson, J. Goddard, D. W. Chipman, and S. C. Sutherland (1993), Seasonal variation of CO₂ and nutrients in the high-latitude surface oceans: A comparative study, *Global Biogeochem. Cycles*, *7*, 843–878, doi:10.1029/93GB02263.
- Takahashi, T., et al. (2002), Global sea-air CO₂ flux based on climatological surface ocean pCO₂, and seasonal biological and temperature effects, *Deep Sea Res., Part II*, *49*, 1601–1622, doi:10.1016/S0967-0645(02)00003-6.
- Ueyama, R., and B. C. Monger (2005), Wind-induced modulation of seasonal phytoplankton blooms in the North Atlantic derived from satellite observations, *Limnol. Oceanogr.*, *50*(6), 1820–1829.
- Ullman, D., G. A. McKinley, V. Bennington, and S. Dutkiewicz (2009), Trends in the North Atlantic carbon sink: 1992–2006, *Global Biogeochem. Cycles*, doi:10.1029/2008GB003383, in press.
- Wanninkhof, R. (1992), Relationship between wind speed and gas exchange over the ocean, *J. Geophys. Res.*, *97*(C5), 7373–7382, doi:10.1029/92JC00188.

V. Bennington, G. A. McKinley, and D. Ullman, Department of Atmospheric and Oceanic Sciences, University of Wisconsin-Madison, 1225 West Dayton Street, Madison, WI 53703, USA. (benesh@wisc.edu)
S. Dutkiewicz, Earth, Atmospheric, and Planetary Sciences, Massachusetts Institute of Technology, 77 Massachusetts Avenue, Cambridge, MA 02139-4307, USA.